ISSN 1948-5204 (online)

World Journal of *Gastrointestinal Oncology*

Monthly Volume 17 Number 4 April 15, 2025

Published by Baishideng Publishing Group Inc

World Journal of Gastrointestinal Oncology

Contents

Monthly Volume 17 Number 4 April 15, 2025

EDITORIAL

REVIEW

ORIGINAL ARTICLE

Case Control Study

Retrospective Cohort Study

Retrospective Study

Clinical Trials Study

Observational Study

Prospective Study

Basic Study

ABOUT COVER

Peer Review of *World Journal of Gastrointestinal Oncology*, Jihwan Ko, MD, FRSPH, Director, Baekyang Jeil Internal Medicine Clinic, Busan 47181, South Korea. jihwanko65@gmail.com

AIMS AND SCOPE

The primary aim of *World Journal of Gastrointestinal Oncology* (*WJGO*, *World J Gastrointest Oncol*) is to provide scholars and readers from various fields of gastrointestinal oncology with a platform to publish high-quality basic and clinical research articles and communicate their research findings online.

WJGO mainly publishes articles reporting research results and findings obtained in the field of gastrointestinal oncology and covering a wide range of topics including liver cell adenoma, gastric neoplasms, appendiceal neoplasms, biliary tract neoplasms, hepatocellular carcinoma, pancreatic carcinoma, cecal neoplasms, colonic neoplasms, colorectal neoplasms, duodenal neoplasms, esophageal neoplasms, gallbladder neoplasms, *etc*.

INDEXING/ABSTRACTING

The *WJGO* is now abstracted and indexed in PubMed, PubMed Central, Science Citation Index Expanded (SCIE, also known as SciSearch®), Journal Citation Reports/Science Edition, Scopus, Reference Citation Analysis, China Science and Technology Journal Database, and Superstar Journals Database. The 2024 edition of Journal Citation Reports® cites the 2023 journal impact factor (JIF) for *WJGO* as 2.5; JIF without journal self cites: 2.5; 5-year JIF: 2.8; JIF Rank: 72/143 in gastroenterology and hepatology; JIF Quartile: Q3; and 5-year JIF Quartile: Q2. The *WJGO*'s CiteScore for 2023 is 4.2 and Scopus CiteScore rank 2023: Gastroenterology is 80/167; Oncology is 196/404.

RESPONSIBLE EDITORS FOR THIS ISSUE

NAME OF JOURNAL
World Journal of Gastrointestinal Oncology

ISSN
ISSN 1948-5204 (online)

LAUNCH DATE
February 15, 2009

FREQUENCY
Monthly

EDITORS-IN-CHIEF
Monjur Ahmed

EDITORIAL BOARD MEMBERS
https://www.wjgnet.com/1948-5204/editorialboard.htm

PUBLICATION DATE
April 15, 2025

INSTRUCTIONS TO AUTHORS
https://www.wjgnet.com/bpg/gerinfo/204

GUIDELINES FOR ETHICS DOCUMENTS
https://www.wjgnet.com/bpg/GerInfo/287

GUIDELINES FOR NON-NATIVE SPEAKERS OF ENGLISH
https://www.wjgnet.com/bpg/gerinfo/240

PUBLICATION ETHICS
https://www.wjgnet.com/bpg/GerInfo/288

PUBLICATION MISCONDUCT
https://www.wjgnet.com/bpg/gerinfo/208

ARTICLE PROCESSING CHARGE
https://www.wjgnet.com/bpg/gerinfo/242

STEPS FOR SUBMITTING MANUSCRIPTS
https://www.wjgnet.com/bpg/GerInfo/239

ONLINE SUBMISSION
https://www.f6publishing.com

World Journal of Gastrointestinal Oncology

Submit a Manuscript: https://www.f6publishing.com

World J Gastrointest Oncol 2025 April 15; 17(4): 99188

DOI: 10.4251/wjgo.v17.i4.99188

ISSN 1948-5204 (online)

ORIGINAL ARTICLE

Basic Study

Impact of SLC16A8 on tumor microenvironment and angiogenesis in colorectal cancer: New therapeutic target insights

Hong-Peng Tian, Zhong-Xiang Xiao, Bo-Wen Su, Yi-Xuan Li, Hong Peng, Chang-Yuan Meng

Specialty type: Oncology

Provenance and peer review: Unsolicited article; Externally peer reviewed.

Peer-review model: Single blind

Peer-review report's classification

Scientific Quality: Grade B, Grade B

Novelty: Grade B, Grade B

Creativity or Innovation: Grade B, Grade B

Scientific Significance: Grade B, Grade B

P-Reviewer: Martin MJ; Wu TT

Received: July 16, 2024

Revised: November 8, 2024

Accepted: January 15, 2025

Published online: April 15, 2025

Processing time: 252 Days and 10.1 Hours

Hong-Peng Tian, Zhong-Xiang Xiao, Bo-Wen Su, Chang-Yuan Meng, Second Department of Gastrointestinal Surgery, The Affiliated Hospital of North Sichuan Medical College, Nanchong 637000, Sichuan Province, China

Yi-Xuan Li, Department of Premarital and Prenatal Examination, Nanchong Shunqing District Maternal and Child Health Hospital, Nanchong 637000, Sichuan Province, China

Hong Peng, Department of Anorectal Surgery, Nanchong Central Hospital, The Second Clinical Medical College, North Sichuan Medical College, Nanchong 637000, Sichuan Province, China

Co-first authors: Hong-Peng Tian and Zhong-Xiang Xiao.

Co-corresponding authors: Hong Peng and Chang-Yuan Meng.

Corresponding author: Hong Peng, Doctor, Department of Anorectal Surgery, Nanchong Central Hospital, The Second clinical Medical College, North Sichuan Medical College, No. 97 Renmin South Road, Shunqing District, Nanchong 637000, Sichuan Province, China. p1041910523@126.com

Abstract

BACKGROUND

SLC16A8, a lactate efflux transporter, is upregulated in various cancers, but its effects on tumor microenvironments remain understudied. This research explores its role in colorectal cancer (CRC) and the impact on the associated microenvironment consisting of vascular endothelial cells.

AIM

To explore the role in CRC and the impact on the associated microenvironment consisting of vascular endothelial cells.

METHODS

Hypoxic conditions prompted examination of SLC16A8 expression, glycolysis, lactate efflux, and Warburg effect correlations in CRC cell lines. Co-culture with HUVEC allowed for endothelial-mesenchymal transition (EndMT) characterization, revealing lactate efflux's influence. Knockdown of SLC16A8 in CRC cells enabled relevant phenotype tests and tumorigenesis experiments, investigating tumor growth, blood vessel distribution, and signaling pathway alterations.

RESULTS
SLC16A8 expression was significantly upregulated in CRC tissues compared to adjacent normal tissues and correlated with disease progression ($P < 0.05$). Under hypoxic conditions, HIF-1α induced SLC16A8 expression, leading to enhanced metabolic reprogramming and increased lactate production. siRNA-mediated SLC16A8 knockdown effectively reversed hypoxia-induced changes, including reduced glucose consumption and lactate production. Co-culture experiments revealed that SLC16A8 knockdown significantly inhibited hypoxia-induced EndMT in HUVEC cells. *In vivo* studies demonstrated that SLC16A8 knockdown suppressed tumor growth, reduced Ki67 expression, and decreased HIF-1α levels. Furthermore, SLC16A8 silencing led to decreased expression of key metabolic enzymes PKM2 and LDHA, indicating its role in glycolytic regulation.

CONCLUSION
Our findings reveal that SLC16A8 functions as a critical mediator of hypoxia-induced metabolic reprogramming in CRC progression.

Key Words: SLC16A8; Colorectal cancer; Hypoxia; Glycolysis; Angiogenesis

Core Tip: Hypoxic SLC16A8 upregulated glycolysis factors in cancer cells. Co-culture with HUVEC increased endothelial-mesenchymal transition in endothelial cells. Knockdown reversed phenotypes in both cell types. *In vivo*, SLC16A8 inhibition reduced tumor growth and angiogenesis, and enhanced apoptosis.

Citation: Tian HP, Xiao ZX, Su BW, Li YX, Peng H, Meng CY. Impact of SLC16A8 on tumor microenvironment and angiogenesis in colorectal cancer: New therapeutic target insights. *World J Gastrointest Oncol* 2025; 17(4): 99188
URL: https://www.wjgnet.com/1948-5204/full/v17/i4/99188.htm
DOI: https://dx.doi.org/10.4251/wjgo.v17.i4.99188

INTRODUCTION

Colorectal cancer (CRC) is a frequent gastrointestinal malignancy worldwide. There were 1.9 million new CRC cases and 935000 deaths in 2020, accounting for 1/10 of all cancers[1,2]. And most cases of CRC are not caused by a single factor[3]. Most patients with CRC have no obvious symptoms in the early stage, and about 40%-50% of patients are already in the advanced stage when diagnosed, who have distant metastases with a 5-year survival rate of only 12.5%[4]. The most familiar sites of metastasis are the liver, peritoneum and lung[5]. Currently, therapy is based on radical surgery and radiotherapy[2,6]. While the recurrence and metastasis rates are high after surgery[7]. Therefore, studying the mechanism of CRC development is beneficial to the accurate diagnosis, precise treatment and early prevention of the disease, which is also is an effective way to reduce CRC mortality.

Cancer cells undergo metabolic reprogramming to promote growth, survival, proliferation and long-term maintenance [8]. A common feature of this metabolic alteration is increased glucose uptake and metabolism of glucose to lactate in the presence of perfectly normal mitochondrial function, a phenomenon known as the Warburg effect, or aerobic glycolysis [9]. In recent years, research on cancer metabolism has progressively delved into understanding how metabolic alterations in tumor cells influence tumor progression[10]. A hallmark of tumor cells is their uncontrolled proliferation. Unlike healthy cells, tumor cells exhibit rapid growth rates and have significantly higher metabolic demands[11]. The metabolic profile of tumor cells causes a substantial depletion of metabolites in the local microenvironment, leading to resource constraints. Besides, waste products produced by tumor cell metabolism may impede the growth of neighboring cells and the production of excess lactate generates an acidic tumor microenvironment that promotes tumor migration and invasion[12]. Therefore, molecules that attenuate the Warburg effect of CRC cells have a key role in the treatment of CRC.

The *SLC16* gene family consists of 14 members, which are also known as the monocarboxylate transporter family[13]. *SLC16* family members are involved in a wide range of metabolic pathways, including energy metabolism, gluconeogenesis, T-lymphocyte activation, intestinal metabolism, spermatogenesis, pancreatic p-cell dysfunction, thyroid hormone metabolism and drug transport in brain, skeletal muscle, heart and tumor cells[14,15]. *SLC16A8*, a member of this gene family, is mainly responsible for the transport of monocarboxylic acid metabolites such as pyruvate, L-lactate and ketone bodies[16]. SLC16A8 also can participate in intercellular lactate transport across membranes. However, it is not clear that SLC16A8 promotes CRC malignant behavior by altering the Warburg effect.

In our study, to investigate the role of SLC16A8 in CRC, we first confirmed the expression and prognosis of SLC16A8 in CRC. Besides, we investigated the impacts of hypoxia on the proliferation, epithelial-mesenchymal transition (EMT), metastasis, glycolysis, and angiogenesis of CRC cells. And we further confirmed the effect of SLC16A8 silencing on these malignant behaviors of CRC under hypoxia condition. This study was conducted to provide potential targets for the therapy and diagnosis of CRC.

MATERIALS AND METHODS

Clinical samples

CRC tissues and paired para-cancerous tissues were collected at Nanchong Central Hospital from January 2022 to December 2023. Inclusion criteria: None of them received radiotherapy or chemotherapy before surgery and post-operative pathological examination was confirmed as CRC. Exclusion criteria: Incomplete medical records; preoperative neoadjuvant therapy; complicated with other systemic malignancies; and severe insufficiency of other organs. All tissues were rapidly stored at -80 °C. All patients signed the informed consent form approved by the ethics committee of Nanchong Central Hospital (approval No. 2023-055). This study complied with medical ethics regulations and the Declaration of Helsinki (Brazil, 2013).

Cell culture, co-culture and treatment

FHC, SW480, RKO, HCT116 and LoVo cell lines were purchased from China National Collection of Authenticated Cell Culture. Briefly, cells were cultured in RPMI-1640 medium with 10% FBS, 1% Penicillin-Streptomycin solution under 37 °C with 5% CO_2. During cell passage, the cells were pre-treated with 0.25% trypsin to digest them into a single-cell suspension, and the digestion reaction was terminated with complete culture medium. The cells were then subcultured at a ratio of 1:3. Co-culturing of CRC cells with HUVEC is conducted using a transwell chamber. During the co-culture process, HUVEC are seeded in the lower chamber, and CRC cells are placed in the upper chamber, maintaining a ratio of 5:1 between the two. The culturing conditions are set at 37°C, 5% carbon dioxide, and 100% humidity.

CRC cells were placed in hypoxia chamber at 0.5% O_2 with a gas mixture consisting of 95% N_2/5% CO_2 for 1, 6, and 12 hours, and cells cultured under 5% O_2 were set as control. SLC16A8 siRNA1 (AGCAGUUGGUGGCGACAGCCAdTdT), SLC16A8 siRNA2 (AGCACAACGCAGGCAGCAGUUdTdT), SLC16A8 siRNA3 (UUAGCACAACGCAGGCAG-CAGdTdT), and NC (AGUUCGGAGACCAGGUGGCCAdTdT) were acquired from GenePharma (Shanghai, China). CRC cells (1×10^3 cells/well) were transfected with the above oligonucleotides by applying lipofectamine 3000 (Invitrogen) for 48 hours based on the specification.

qRT-PCR

For clinical tissues, they were ground into powder after treatment with liquid nitrogen, followed by total RNA extraction using Trizol reagent. For cells, they were directly lysed using Trizol solution. The extraction process was conducted according to the manual. RNA concentration was quantified using a NanoDrop spectrophotometer, and 1 μg of total RNA was reverse transcribed to obtain a cDNA template. Specific primers were used, and real-time PCR was performed using SYBR Green to obtain the Ct values of each sample. The relative mRNA expression levels in each sample were calculated using the $2^{-\Delta\Delta Ct}$ method. ACTB was used as an internal reference in this experiment. The primers' sequences were listed in Table 1.

Cell proliferation

For the CCK-8 assay, CRC cells (4×10^5 cells/mL) were seeded in 96-well plates and transfected for 48 hours according to the experimental design. Subsequently, 10 μL of CCK-8 reagent (Dojindo, Tokyo, Japan) was added to each well. After a 2-hour incubation period, the optical density (OD) value at 450 nm was measured. Cells (approximately 1×10^5 cells) were subjected to hypoxia or siRNA treatment for 48 hours, followed by detection using the EdU staining kit provided by Beyotime (Shanghai, China). Briefly, EdU solution was added to the cells and then incubated for an additional 2 hours. Subsequently, the EdU staining solution was discarded, and the cells were fixed with paraformaldehyde and permeabilized with Triton X-100. The fluorescent detection solution was added, followed by a 30-minute incubation in the dark at room temperature. Finally, DAPI nuclear staining solution was added to stain the cell nuclei, and the proliferative activity signals were observed under a laser confocal microscope.

Transwell

Cell migration and invasion capacities were assessed using Transwell chambers (8 μm pore size, Corning). For migration analysis, CRC cells were harvested and suspended in serum-free medium at a density of 5×10^4 cells per well. The cells were seeded in the upper chamber, while the lower chamber contained 500 μL complete medium supplemented with 10% FBS as a chemoattractant. Following 24-hour incubation under standard conditions, non-migrated cells were removed from the upper surface using cotton swabs. The migrated cells were fixed with 4% paraformaldehyde (20 minutes), stained with 1% crystal violet (10 minutes), and quantified by counting five random microscopic fields. For invasion assays, the upper chambers were pre-coated with Matrigel (EMD Millipore; Cat. No. 356234, diluted 1:8 in serum-free medium). Briefly, 80 μL of diluted Matrigel was applied to each insert and allowed to polymerize at 37 °C for 1 hour. The subsequent experimental procedures were identical to the migration assay protocol.

Tube formation assay

In this study, to evaluate the impact of CRC cells on endothelial cell angiogenesis, HUVECs were co-cultured with CRC cells, and their tube formation ability was assessed using a tube formation assay. Matrigel was thawed overnight in advance at 4 °C in the refrigerator, and was diluted with FBS-free medium. The cells were inoculated with 2×10^5 cells/well on the surface of the Matrigel at 37 °C for 24 hours. After a few hours, cells begin to form capillary-like structures. The results were recorded by an inverted microscopy. The degree of tube formation is then quantified by counting the number of tubes or measuring the total tube length under a microscope.

Table 1 The primers' sequences

Name	Sequence (5'-3')	Product length (bp)
ACTB F	CATGTACGTTGCTATCCAGGC	154
ACTB R	CTCCTTAATGTCACGCACGAT	
SLC16A8 F	TGCCTGCGTTGTGCTAAAG	119
SLC16A8 R	GGTTCCTCTGCAACAACAGG	

Determination of glucose consumption

In this experiment, a glucose uptake assay kit provided by Abcam was utilized. Briefly, after subjecting cells to hypoxia or siRNA transfection, they underwent starvation treatment. Subsequently, cells were incubated with 2-deoxyglucose (2-DG), a glucose analog, with or without insulin stimulation. Cells were then lysed to measure the intracellular 2-DG content. The concentration of 2-DG6P was quantified by measuring the absorbance at $OD_{412\ nm}$ in the lysate. A standard curve for 2-DG6P was established prior to the experiment based on standard samples.

lactate concentration detection

To perform the L-lactate assay, an L-lactate assay kit (abcam, ab65331) was used. Cells were harvested (approximately 2 × 10^6 cells), and washed with cold PBS, and homogenize by pipetting. Afterwards, homogenate was centrifuge at 4 °C for 5 minutes to remove insoluble material, then keep the supernatant on ice. The endogenous lactate dehydrogenase was removed using Deproteinizing Sample Preparation Kit – TCA (ab204708). Then 50 µL of reaction mix per reaction was prepared, following the provided amounts for assay buffer, developer solution, and enzyme mix. Besides, standard wells were set up with 50 µL of standard dilutions and sample wells with 2-50 µL of samples, adjusted to 50 µL with lactate assay buffer. Incubate the plate at room temperature for 30 minutes and measure at $OD_{450\ nm}$. Calculate concentrations by comparing with the standard curve, adjusted for any sample dilution.

Detection of ECAR

After hypoxia or siRNA transfection, cells were seeded into a 96-well Seahorse microplate (cell density 2 × 10^4/mL), at 80 µL per well, and cultured at 37 °C in a 5% CO_2 incubator for 16 hours. The calibration plate was equilibrated overnight in a non-CO_2 incubator. Prior to measurement, cells were washed twice with assay medium and equilibrated in a non-CO_2 incubator. After calibration, the probe plate was replaced with the cell plate. For the ECAR measurement, glucose (10 mmol/L), oligomycin (1 µmol/L), and 2-DG (100 mmol/L) were sequentially injected, and measurements were taken continuously.

Western blot

The total protein was harvested *via* RIPA lysate (Beyotime, China), and was monitored by BCA kit (Invitrogen). Proteins (40 µg) were separated in SDS-PAGE gel, transferred to PVDF membrane (Millipore). After blocking, the membranes were exposed to primary antibody, PKM2 (Boster, PB9379, 1:1000), LDHA (Boster, PB10075, 1:1000), E-cadherin (Boster, PB9561, 1:1500), N-cadherin (Boster, BA0673, 1:2000), Vimentin (Boster, BM0135, 1:1000), SLC16A8 (antibodies-online, ABIN630366, 2.5 µg/mL), ACTB (Boster, BA2305, 1:5000) overnight at 4 °C. Afterwards, membranes were treated with a secondary antibody (Abcam, ab7090, 1:5500) for 1 hour, followed by dropwise addition of ECL color development solution for visualization. After ECL chemiluminescence, protein was developed on the gel imager (Bio-rad). ACTB was used as internal reference.

In vivo xenograft modeling

Nude mice (6 weeks old, half male and half female, 20 g) were provided by the Animal Experiment Center of Nanchong Central Hospital, with 5 mice per group. After expansion, LoVo cells were injected subcutaneously into the mice, with each mouse receiving an injection of 5 × 10^6 cells. Subsequently, siRNA was injected every other day at a dose of 15 nmol/20 g *via* intravenous injection. During the experiment, the animals were provided with sufficient water and food, the animal laboratory was maintained at 23 ± 2 °C, and the humidity was kept at 60%. The experiment lasted for 4 weeks. The length and width of the tumor were measured weekly, and the tumor volume was calculated using the formula (volume = length × width^2 × 0.5). After anesthesia with sodium pentobarbital, the animals were quickly euthanized by cervical dislocation. Tumor tissues were collected for subsequent experimental testing. Ethical approval for all animal experimental procedures was provided by the Animal Ethics Committee of Nanchong Central Hospital.

H&E staining

Tumors from mice were processed through 4% paraformaldehyde fixation, gradient ethanol dehydration, and embedded in paraffin blocks for 4-µm sectioning. After baking, the sections were dewaxed and hydrated with xylene and gradient alcohol, followed by hematoxylin-stained nuclei, eosin-stained cell pulp, ethanol dehydration and xylene transparency, and finally sealed with neutral resin. Morphological changes in tumor tissue were observed under the microscope.

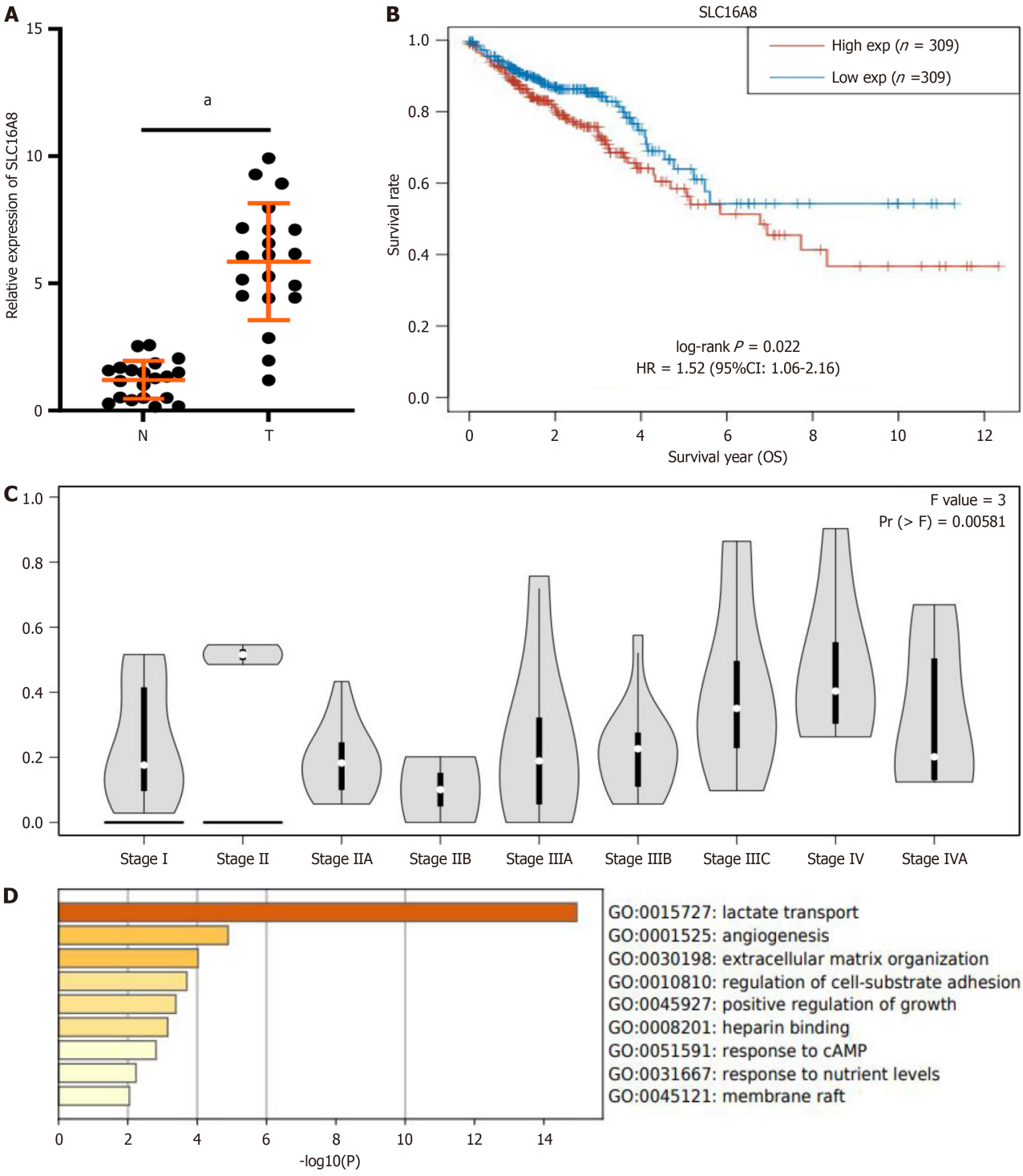

Figure 1 The expression characteristics of SLC16A8 in colorectal cancer. A: The difference in the expression of SLC16A8 in colorectal cancer (CRC) tissues and adjacent tissues; B: The correlation between SLC16A8 and the prognosis of patients with CRC; C: SLC16A8 expression feature varying with stage of CRC; D: Pathways enriched in relation to SLC16A8. $^{a}P < 0.01$. OS: Overall survival.

Immunohistochemistry assay

Paraffin sections were subjected to microwave antigen thermal repair using 0.01 mol/L sodium citrate, and endogenous enzymes were blocked by incubation with 3% H_2O_2. After washing, the sections were closed by 5% BSA for 30 minutes, incubated with the diluted primary antibody (Ki-67, Abcam) at 4 °C overnight, and goat secondary antibody (Abcam) for 1 hour. Then the sections were developed with DAB (Invitrogen, Cat. No. 34002), re-stained with hematoxylin, and sealed with neutral resin. Then the staining results were observed under a microscope. And five high magnification fields (× 200) were selected for each mouse for immunohistochemistry analysis.

Statistical analysis

For Figure 1A, significance testing was performed using the *t*-test method. For experiments involving three or more

groups, a post-hoc analysis followed by Tukey's test was employed. Data visualization was represented in the form of mean ± SD, and GraphPad (Ver 9) was used for the creation of bar graphs and line charts. Data significance analysis was conducted using SPSS 22.0. A P value of < 0.05 was considered statistically significant. Each experiment was repeated three times.

RESULTS

Expression of SLC16A8 in CRC

To analyze the expression characteristics of SLC16A8 in CRC, cancerous and adjacent non-cancerous tissues were collected from patients during surgery, and qPCR experiments were conducted. As shown in Figure 1A, SLC16A8 was significantly upregulated in cancerous tissues, exhibiting a marked difference compared to expression in adjacent non-cancerous tissues. Further database analysis revealed that low SLC16A8 expression was associated with favorable prognosis and survival in CRC patients, demonstrating a significant correlation (Figure 1B). Moreover, as CRC progresses, the expression level of SLC16A8 significantly increases (Figure 1C). Additional pathway analysis indicated that the SLC16A8 gene was closely related to lactate transport and angiogenesis (Figure 1D). These results suggested that the upregulation of SLC16A8 in CRC tissues was associated with disease progression and might indicate a poor prognosis.

HIF-1α promotes SLC16A8 expression and induces metabolic reprogramming in CRC cells

HIF-1α is a crucial transcription factor that regulates cellular responses under hypoxic conditions, and its role in modulating SLC16A8 expression is pivotal for understanding the metabolic reprogramming in CRC cells. This linkage helps elucidate how hypoxic tumor microenvironments can drive the Warburg effect and influence tumor progression. In order to determine the mechanism of action of SLC16A8 and HIF-1α in CRC, the expression level of SLC16A8 in four CRC cell lines (SW480, RKO, HCT116 and LoVo) and the normal fetal human colon epithelial cell line (FHC) was detected by qPCR method. The results are shown in Figure 2A. SLC16A8 is highest expressed in LoVo and RKO cell lines (Figure 2A). Subsequently, LoVo and RKO cell lines were subjected to hypoxia, SLC16A8 and HIF-1α reached their maximum at 6 hours (Figure 2B). Hypoxia for 6 hours was selected for subsequent experiments. The results showed that the extracellular acidification rate of CRC cell lines was significantly increased after hypoxia (Figure 2C). The lactate detection experiment also showed that the extracellular lactate level gradually increased with the increase of hypoxia time (Figure 2D). Western blot results showed that the expression of key enzymes PKM2 and PDHA in metabolic reprogramming increased gradually with hypoxia time (Figure 2E). At the same time, glucose consumption gradually increased (Figure 2F). In summary, HIF-1α promoted the expression of SLC16A8 under hypoxic conditions, further inducing metabolic reprogramming in CRC cells, which had significant implications for tumor energy metabolism.

Hypoxia induce EMT in CRC cells

To determine the malignant biological behavior of CRC cell lines RKO and LoVo under hypoxia, we examined their effects on HUVEC cells under different hypoxia times. As shown in Figure 3A and B, cell proliferation activity of HUVEC cells was significantly enhanced with prolonged hypoxia when co-cultured with RKO and LoVo cells, and positively correlated with time (Figure 3A and B). Further Transwell chamber experiments showed that hypoxia also enhanced the migration and invasion abilities of HUVEC cells in the presence of RKO and LoVo cells (Figure 3C and D). The results demonstrated that the angiogenesis ability of the corresponding HUVEC cells was gradually enhanced with prolonged hypoxia when co-cultured with CRC cells (Figure 3E).and caused the upregulation of N-Cadherin, Vimentin expression and a decreasing of E-cadherin levels (Figure 3F). These data demonstrated that hypoxic conditions significantly enhanced the migration, invasion, and angiogenesis abilities of co-cultured HUVEC cells, suggesting that SLC16A8 might have played a critical role in promoting EMT.

Effective siRNA screen for SLC16A8

In order to further explore the mechanism of SLC16A8 in CRC cells, siRNAs targeting SLC16A8 were designed and synthesized. After transfection of SLC16A8 siRNA into RKO and LoVo cells, qPCR and Western blot results showed that all three siRNAs inhibited SLC16A8 expression. Among them, siRNA 2 had the highest knockdown efficiency (Figure 4A and B), so siRNA 2 was selected for subsequent experiments. Results also showed that the SLC16A8 expression increased with duration of hypoxia (Figure 4C). These findings identified the most effective siRNA for SLC16A8 knockdown, providing a tool for subsequent studies.

SLC16A8 siRNA reverses hypoxia-induced metabolic reprogramming

To clarify the regulation of hypoxia on SLC16A8-mediated tumor metabolic reprogramming, SLC16A8 was further interfered in CRC cells treated with hypoxia. As shown in Figure 5A, SLC16A8 siRNA significantly suppressed the upregulation of SLC16A8 expression induced by hypoxia. The results of extracellular acidification rate showed that the extracellular acidification induced by hypoxia was mitigated by SLC16A8 siRNA (Figure 5B), accompanied by a significant pullback of extracellular lactate content (Figure 5C). Meanwhile, the significant up-regulation of PKM2 and LDHA expression induced by hypoxia was also reversed by SLC16A8 siRNA (Figure 5D), and glucose consumption was inhibited (Figure 5E). The application of SLC16A8 siRNA effectively reversed hypoxia-induced metabolic reprogramming, indicating that SLC16A8's role in regulating CRC cell metabolism could serve as a therapeutic target.

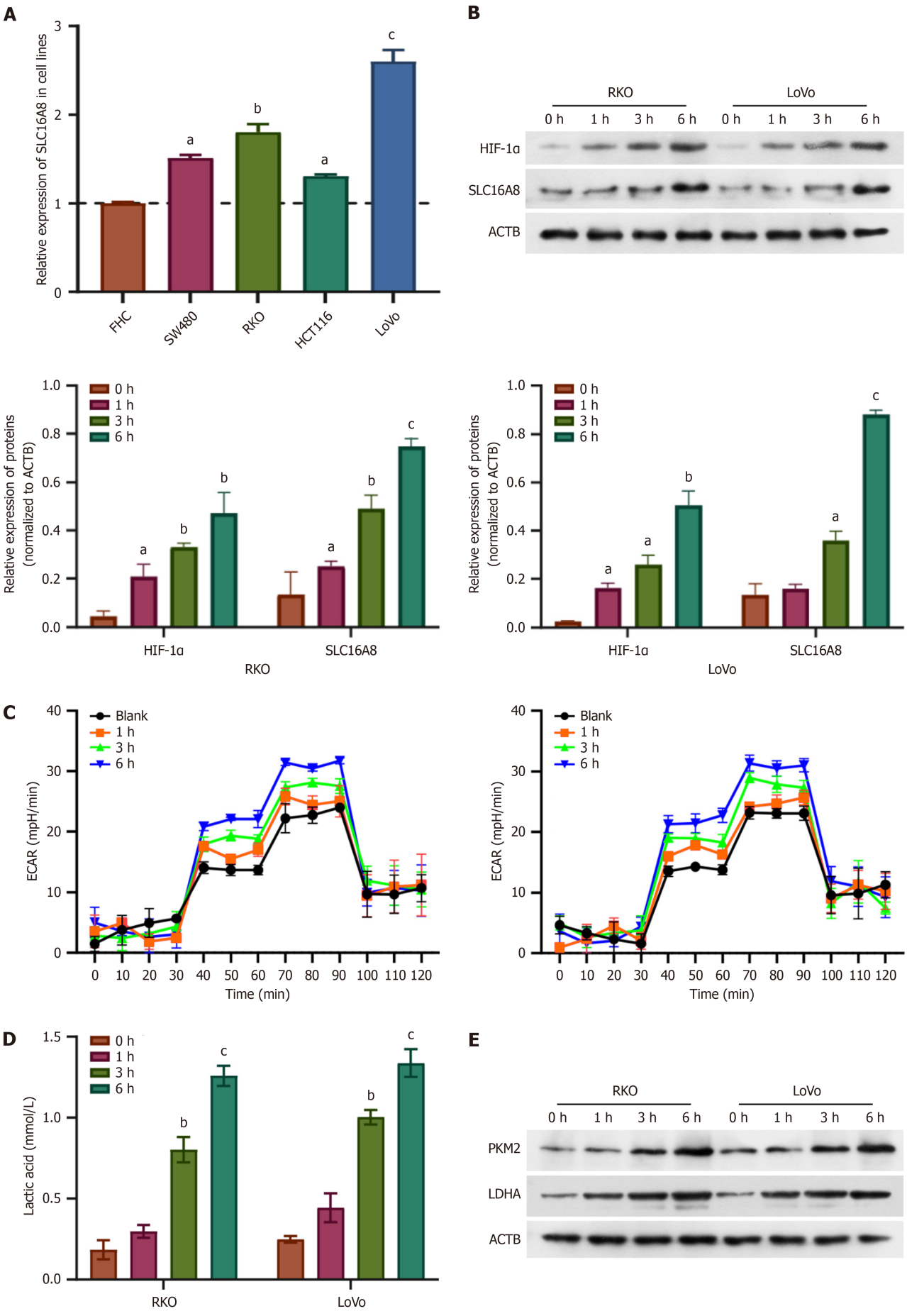
A
Relative expression of SLC16A8 in cell lines
FHC
SW480
RKO
HCT116
LoVo
B
RKO
LoVo
0 h
1 h
3 h
6 h
HIF-1α
SLC16A8
ACTB
Relative expression of proteins (normalized to ACTB)
RKO
LoVo
C
Blank
ECAR (mpH/min)
Time (min)
D
Lactic acid (mmol/L)
E
PKM2
LDHA

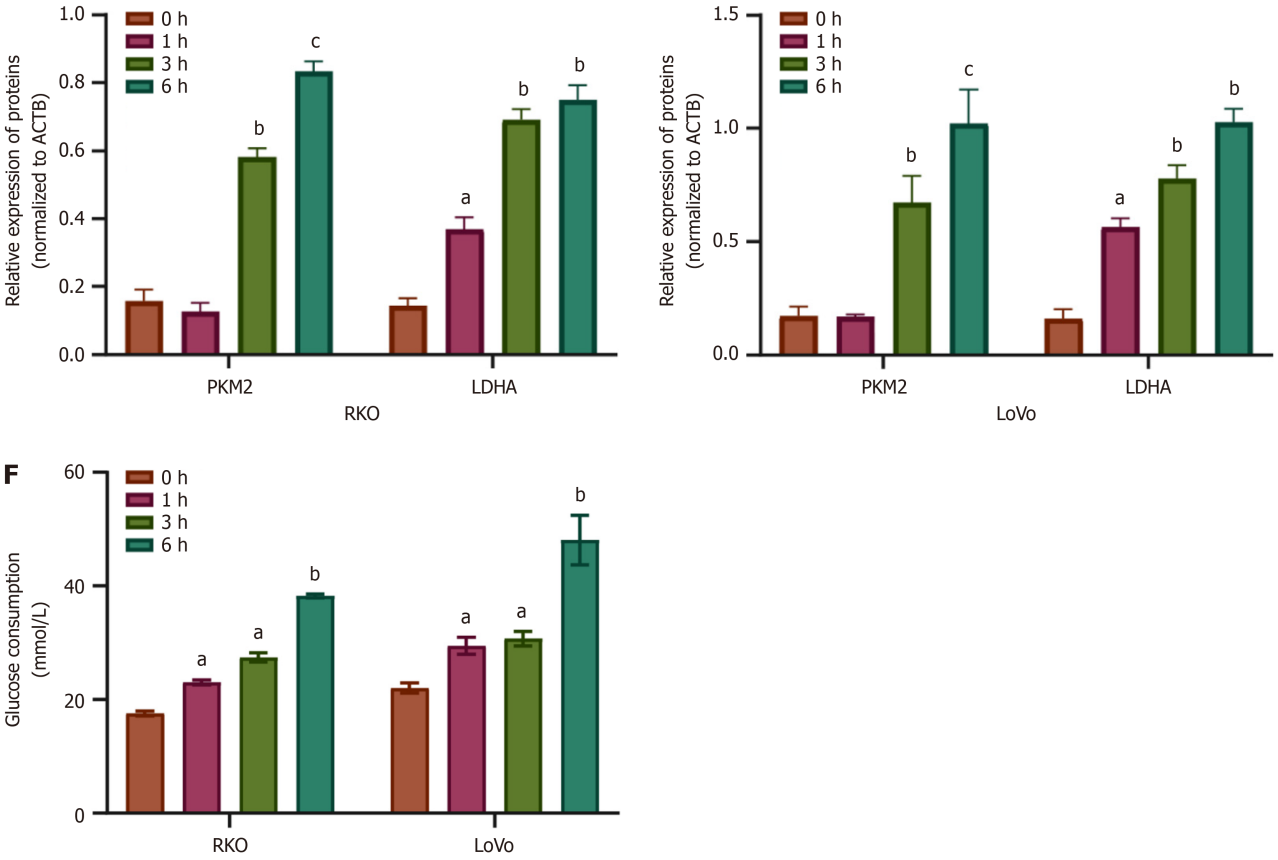

Figure 2 Effects of hypoxia on SLC16A8 expression and metabolic reprogramming of colorectal cancer cells. A: The expression level of SLC16A8 in colorectal cancer cell lines; B: The expression characteristics of SLC16A8 under hypoxia; C: The effect of hypoxia on the ECAR of RKO and LoVo; D: The effect of hypoxia on the extracellular lactate levels of RKO and LoVo; E: The effect of hypoxia on the expression of PKM2 and LDHA, the key proteins of metabolic reprogramming; F: The effect of hypoxia on glucose consumption in RKO and LoVo cells. $^{a}P < 0.05$, $^{b}P < 0.01$, $^{c}P < 0.001$.

Reversal of hypoxia-induced EMT by SLC16A8 siRNA

In order to unveil the mechanism of SLC16A8 in CRC, CRC cells under hypoxic conditions were subjected to SLC16A8 knockdown, co-cultured with HUVEC cells, and the occurrence of endothelial-mesenchymal transition (EndMT) in HUVEC cells was examined. The results showed that SLC16A8 siRNA significantly inhibited the increase in proliferative activity induced by hypoxia in HUVEC cells when co-cultured with RKO and LoVo cells (Figure 6A and B). Transwell chamber experiments showed that the hypoxia-induced enhancement of migration and invasion of HUVEC cells in the presence of RKO and LoVo cells was significantly reversed by SLC16A8 siRNA (Figure 6C and D), accompanied by changes in E-Cadherin, N-Cadherin, and Vimentin expression (Figure 6E). Finally, after the CRC cells of each group were co-cultured with vascular endothelial cells (HUVEC), the results were as shown in Figure 6F. Hypoxia-induced CRC cells could significantly induce vascular endothelial cells (HUVEC) to form tubes; In contrast, SLC16A8 siRNA treatment of CRC cells significantly reversed the ability of endothelial cells (HUVEC) to form tubes (Figure 6F). SLC16A8 siRNA effectively inhibited the EMT induced by hypoxia in CRC cells, highlighting the role of SLC16A8 in the tumor microenvironment.

Impact of SLC16A8 knockdown on tumor in vivo

In order to investigate that effect of SLC16A8 on the growth of tumor, the nude mice bearing tumor model was established. As shown in Figure 7, SLC16A8 knockdown significantly suppressed tumor growth (Figure 7A and B) and significantly suppressed tumor volume (Figure 7C). There was a significant decrease in the Ki67 proliferation index (Figure 7D), indicating reduced tumor cell proliferation. Knockdown of SLC16A8 also led to a marked reduction in HIF-1α expression, as shown in Figure 7E and F. Additionally, apoptosis levels increased (Figure 7G), along with notable histological changes (Figure 7H). The study found that the knockdown of SLC16A8 significantly reduced the lactate levels in animal serum (Figure 7I). Simultaneously, changes in the expression of proteins related to the Warburg effect and EndMT in the tissues were observed (Figure 7J and K). The knockdown of SLC16A8 suppressed *in vivo* tumor growth and glycolysis, emphasizing its potential as a therapeutic intervention target in CRC.

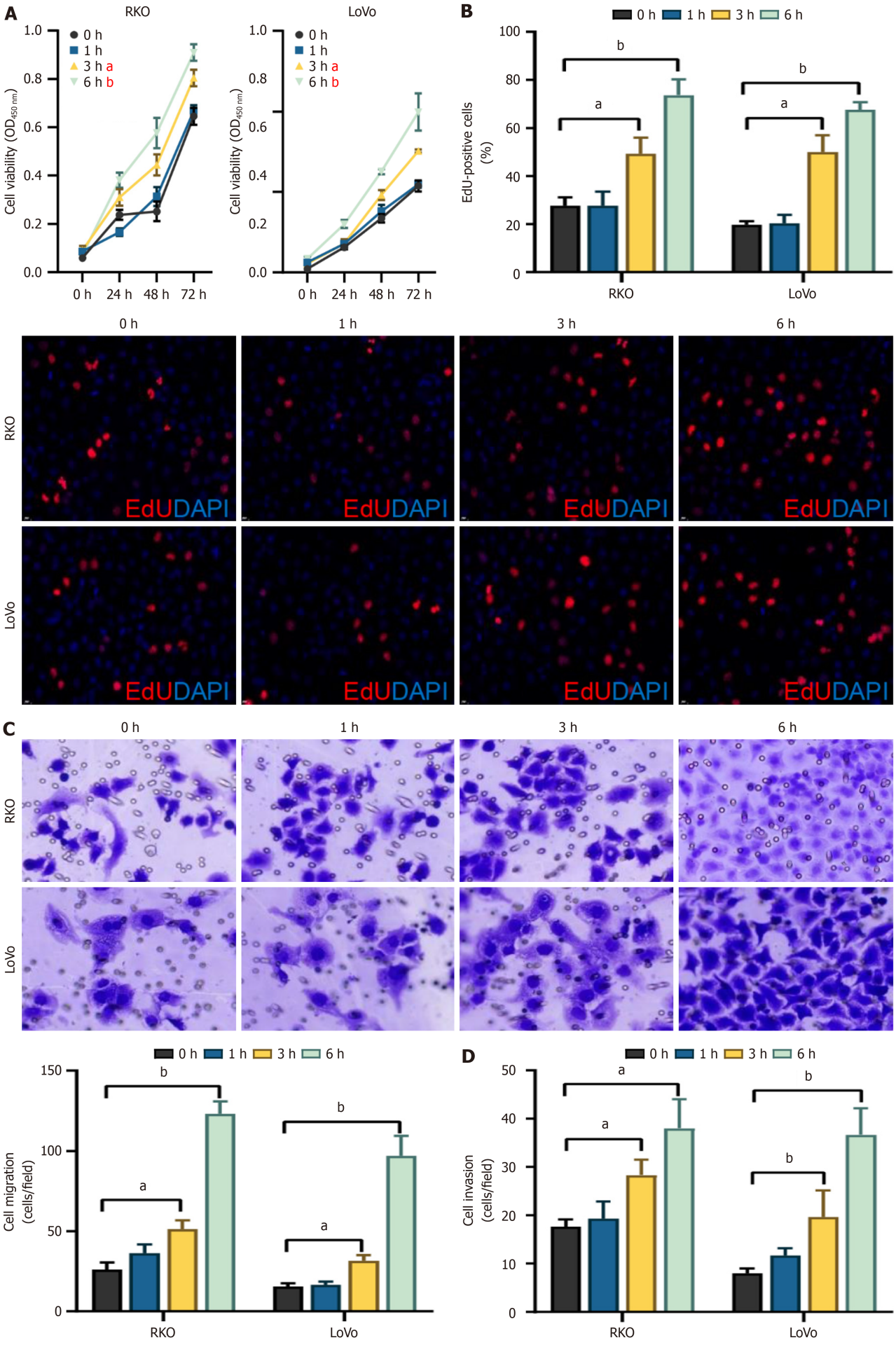
A
RKO
LoVo
0 h
1 h
3 h a
6 h b
Cell viability (OD450 nm)
0 h
24 h
48 h
72 h
B
0 h
1 h
3 h
6 h
EdU-positive cells (%)
a
b
RKO
LoVo
C
0 h
1 h
3 h
6 h
RKO
LoVo
EdUDAPI
Cell migration (cells/field)
D
Cell invasion (cells/field)

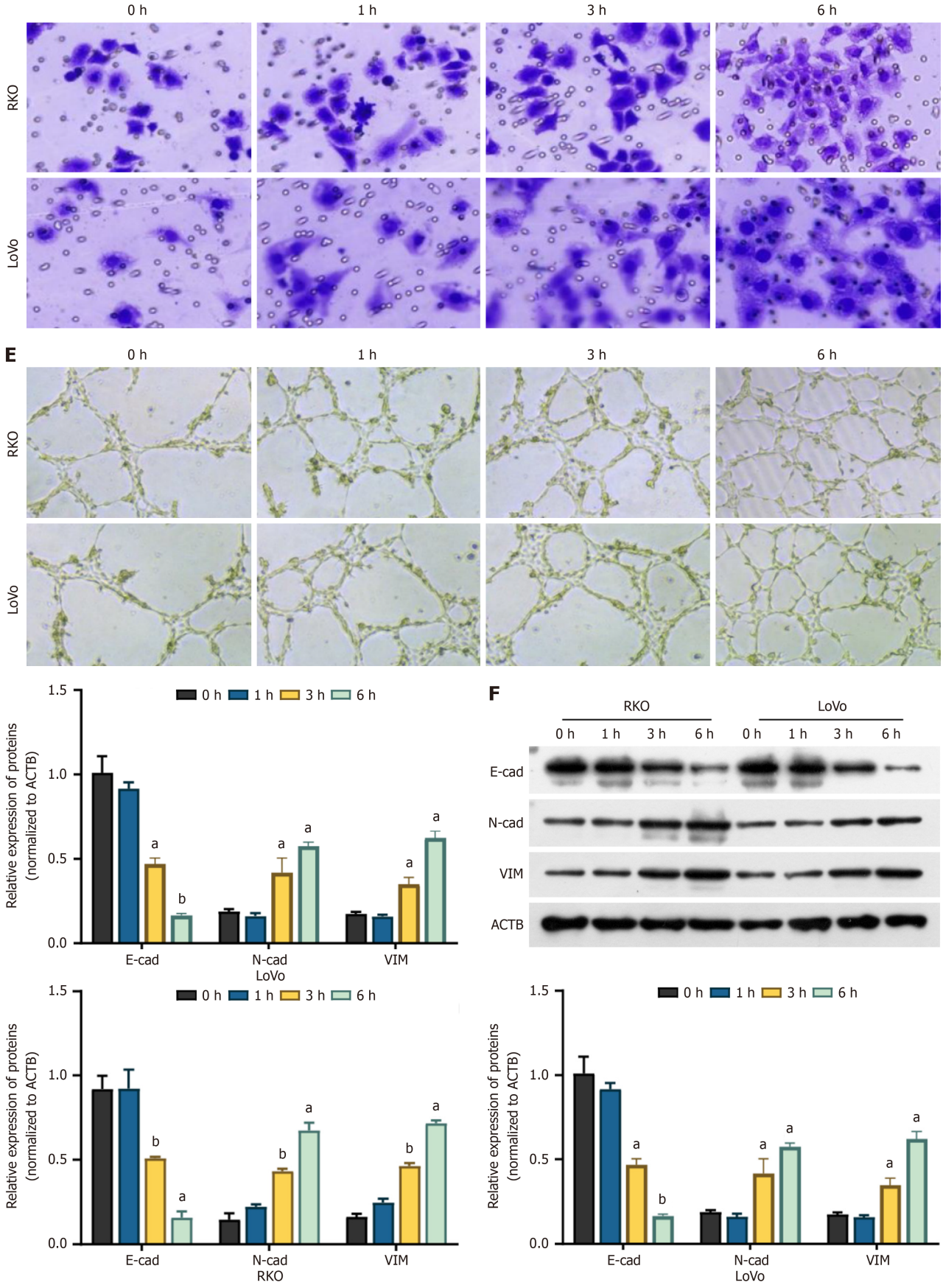

Figure 3 Effect of hypoxia on endothelial-mesenchymal transition of HUVEC co-cultured with colorectal cancer cells. A and B: Effect of hypoxia on cell viability; C and D: Effect of hypoxia on migration (C) and invasion (D) of HUVECs; E: Effect of hypoxia on the ability of endothelial cells' tube formation; F: Hypoxia affected the expression of E-cadherin, N-cadherin and Vimentin in HUVECs. $^{a}P < 0.05$, $^{b}P < 0.01$.

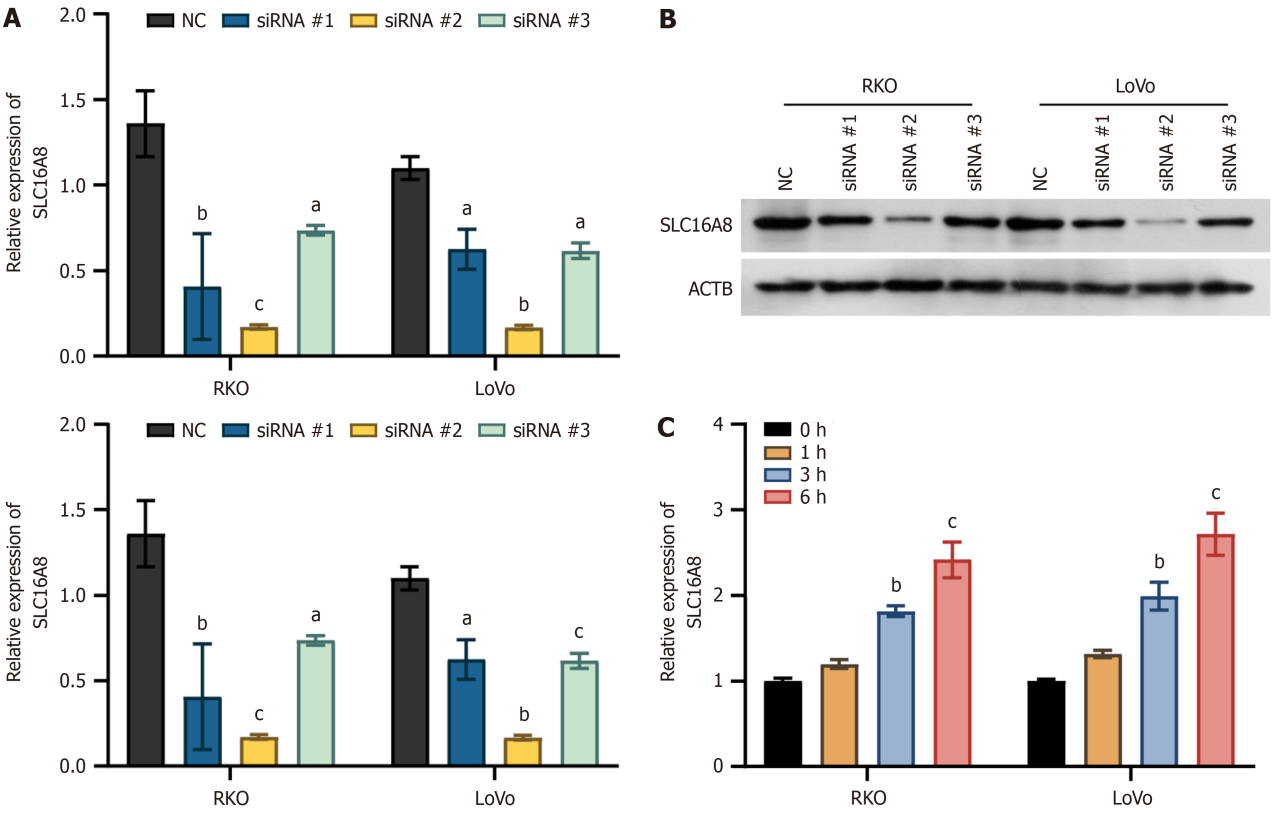

Figure 4 the knock-down efficiency of SLC16A8 siRNAs. A and B: qRT-PCR (A) and Western blot (B) methods were used to screen the siRNA with the highest knockdown efficiency; C: SLC16A8 expression was elevated to hypoxia condition. $^{a}P < 0.05$, $^{b}P < 0.01$, $^{c}P < 0.001$.

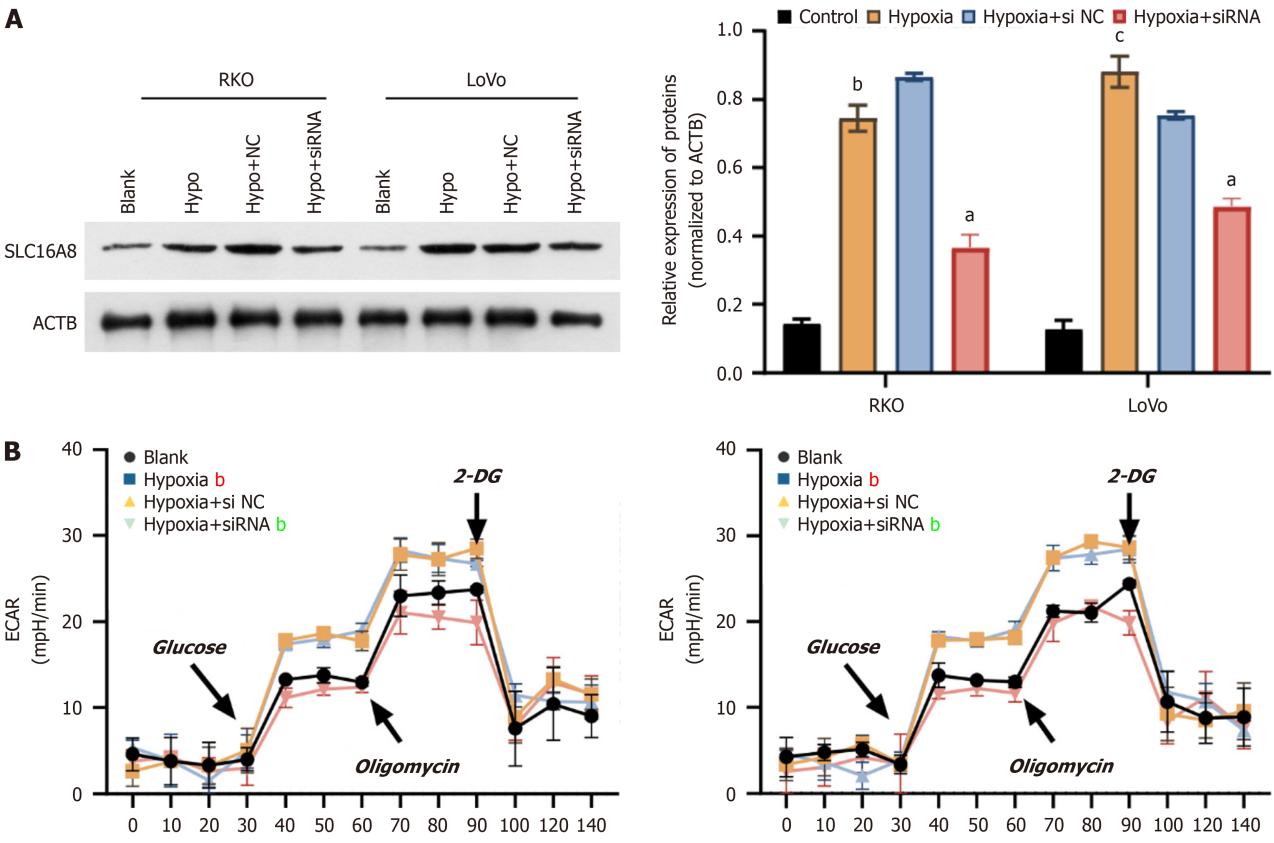

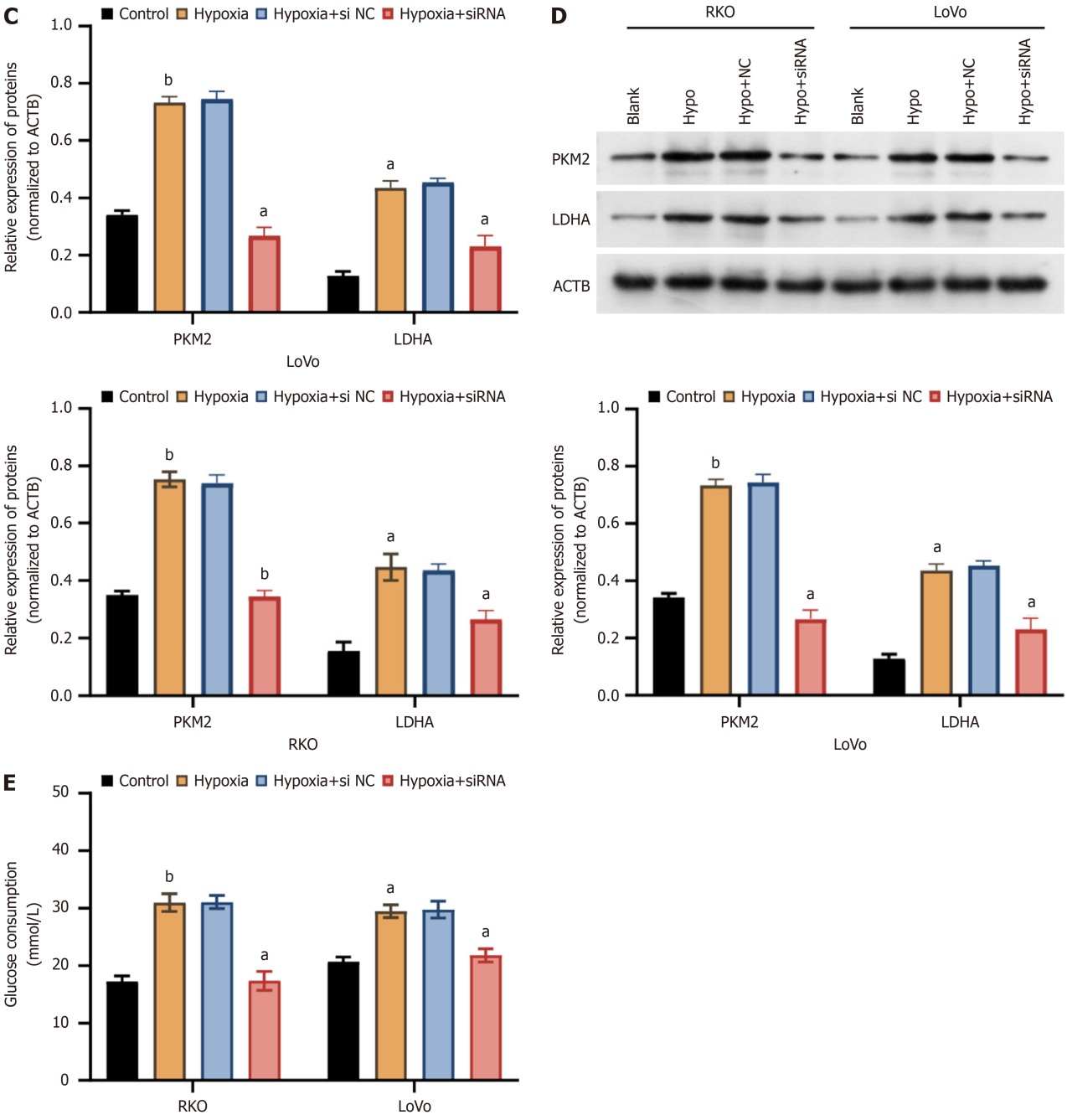

Figure 5 SLC16A8 siRNA reverses the effects of hypoxia on cell metabolic reprogramming. A: SLC16A8 siRNA affects the expression of SLC16A8 in hypoxia treated cells; B: Effect of SLC16A8 siRNA on ECAR of hypoxia treated cells; C: SLC16A8 siRNA can affect the level of extracellular lactic acid after hypoxia treatment; D: SLC16A8 siRNA affects the expression of PKM2 and LDHA in hypoxia treated cells; E: Effect of SLC16A8 siRNA on glucose consumption in hypoxia treated cells. $^{a}P < 0.05$, $^{b}P < 0.01$, $^{c}P < 0.001$. 2-DG: 2-deoxyglucose.

DISCUSSION

CRC is a frequent malignant tumor of the gastrointestinal tract, and its incidence is on the rise year by year[17]. Most patients with CRC are already in the progressive stage at the time of diagnosis[17]. For this group of patients, surgery and adjuvant therapy have limited effectiveness and high adverse effects, leading to poor prognosis[18]. Understanding the molecular mechanisms that drive CRC development and progression remains crucial for advancing therapeutic strategies.

Tissue hypoxia affects tumor metabolism, angiogenesis and intrinsic immunity, and is also considered one of the important microenvironmental factors that promote tumor metastasis[19]. Hypoxia, or reduced oxygen availability, is a common feature of the tumor microenvironment[20]. It affects angiogenesis and metabolism and promotes tumorigenesis and progression[21]. Study have also shown that under hypoxic conditions, CRC cells exhibit resistance to multiple therapeutic agents and enhanced angiogenesis and EMT capacity[22]. Thus, the hypoxic microenvironment is essential for tumor growth. In our study, we proved that hypoxia could enhance CRC cell proliferation, migration, invasion, angiogenesis, EMT suggesting that hypoxia can accelerate the malignant process of CRC.

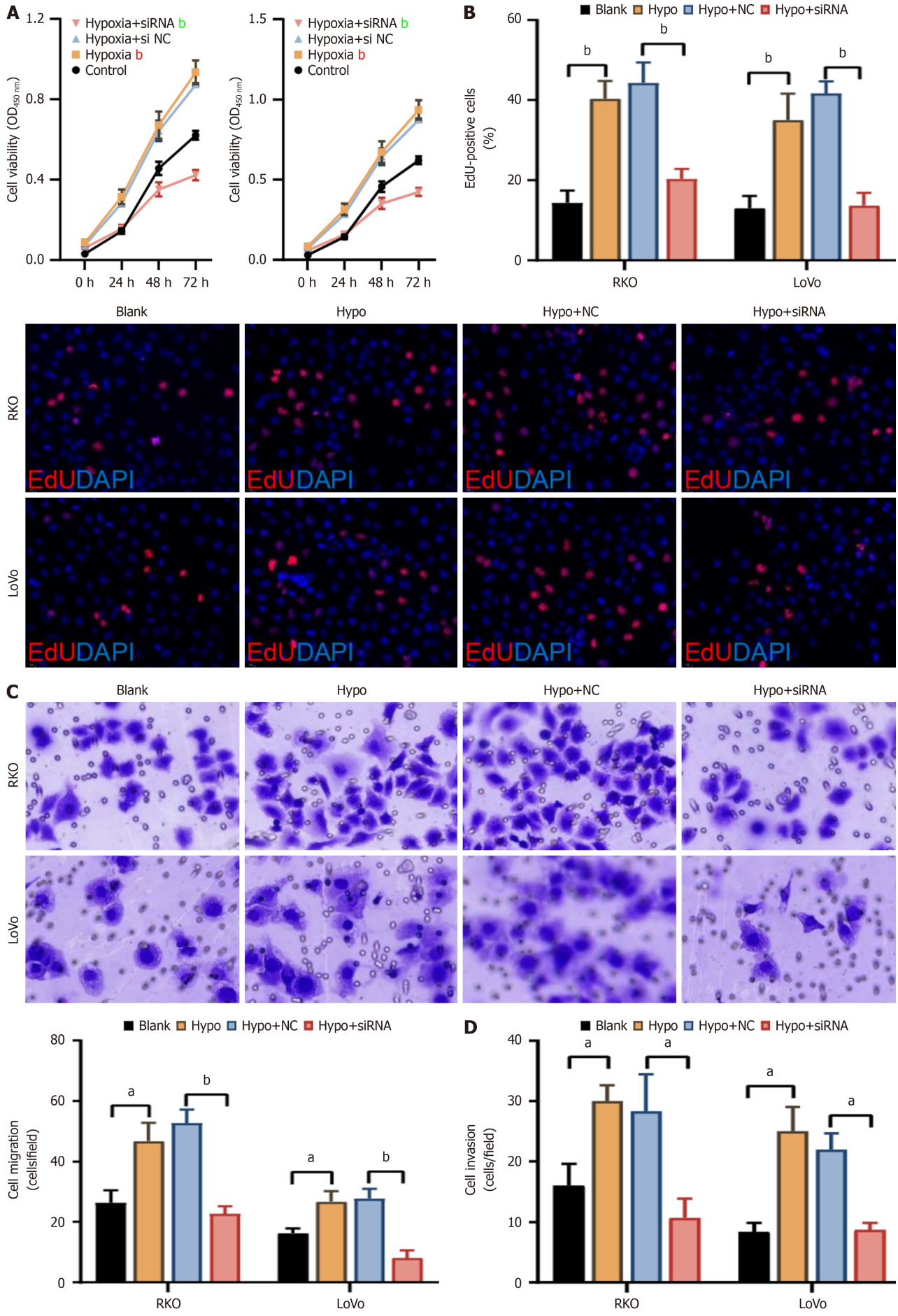
A
Hypoxia+siRNA b
Hypoxia+si NC
Hypoxia b
Control
Cell viability (OD450 nm)
0 h
24 h
48 h
72 h
B
Blank
Hypo
Hypo+NC
Hypo+siRNA
EdU-positive cells (%)
RKO
LoVo
EdU
DAPI
C
Cell migration (cells/field)
D
Cell invasion (cells/field)

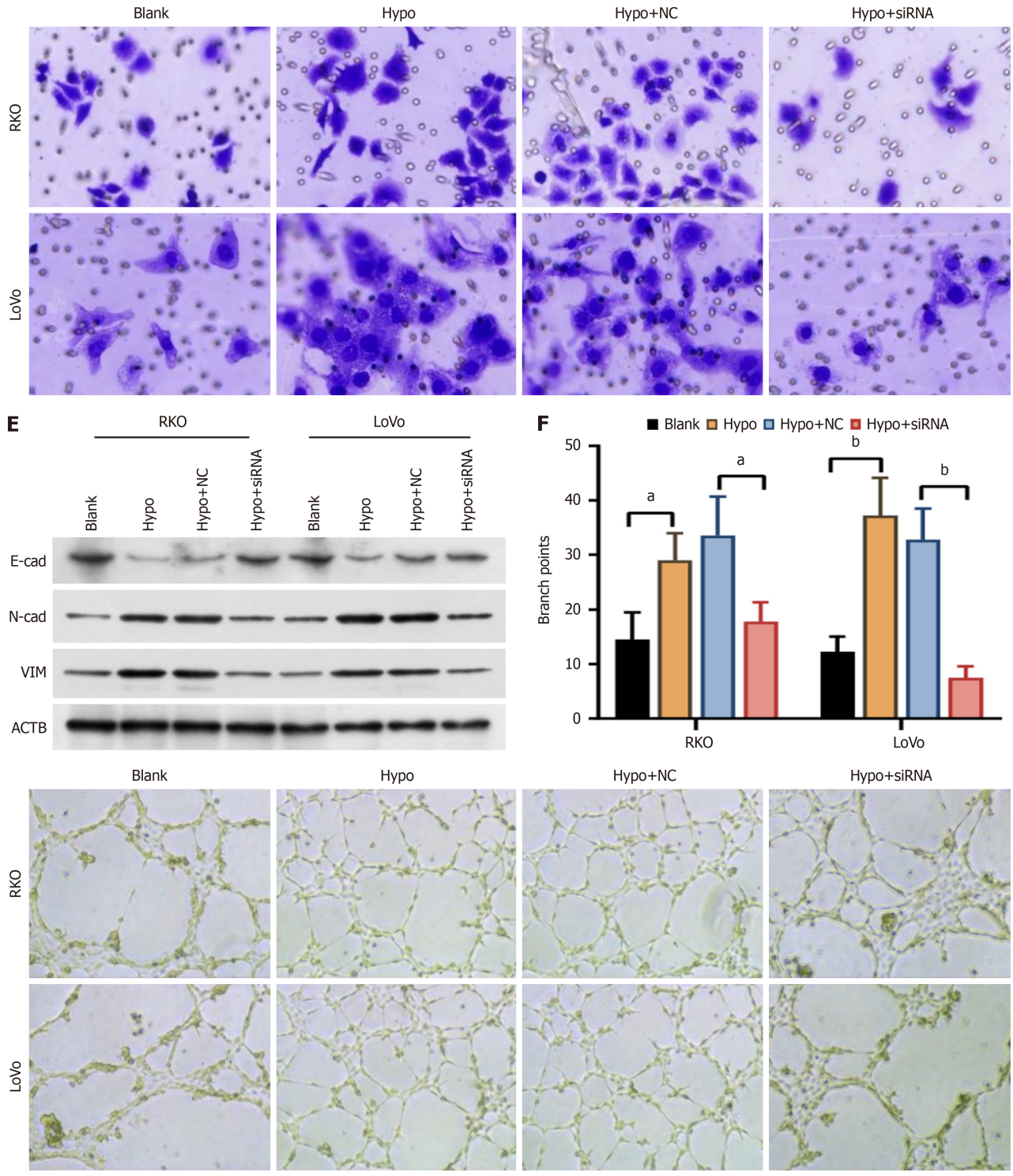

Figure 6 SLC16A8 siRNA reverses the effects of hypoxia on cell endothelial-mesenchymal transition of HUVECs. A and B: The effect of SLC16A8 siRNA on the proliferation of hypoxia treated cells; C and D: SLC16A8 siRNA can affect the migration (C) and invasion (D) of hypoxic HUVECs; E: SLC16A8 siRNA can affect the expression level of E-cadherin, N-cadherin and Vimentin in hypoxia treated cells; F: Effect of SLC16A8 siRNA on the ability of endothelial cells to form tubes after co culture of colorectal cancer cells with hypoxia. $^{a}P < 0.05$, $^{b}P < 0.01$.

The main energy source for tumor cell growth metabolism is glucose metabolism[23]. The body metabolizes glucose primarily through two pathways: oxidative phosphorylation and glycolysis. Research has demonstrated that glycolysis plays a significant role in modulating tumor cell behavior[24]. Glucose enters the cell through membrane-bound glucose transporters and is converted to pyruvate through the process of glycolysis[25]. Under hypoxic conditions, pyruvate is converted to lactate, while in aerobic conditions, it undergoes mitochondrial oxidative phosphorylation to generate energy. The metabolic activity of tumor cells is directly linked to this energy production[26]. Even in the presence of adequate oxygen, tumor cells exhibit a preference for increased glucose consumption and energy production through glycolysis - a phenomenon known as the Warburg effect[27]. Our findings showed that hypoxia increased glucose uptake and lactate production in CRC cells. Additionally, hypoxia elevated ECAR in CRC cells, confirming that hypoxia

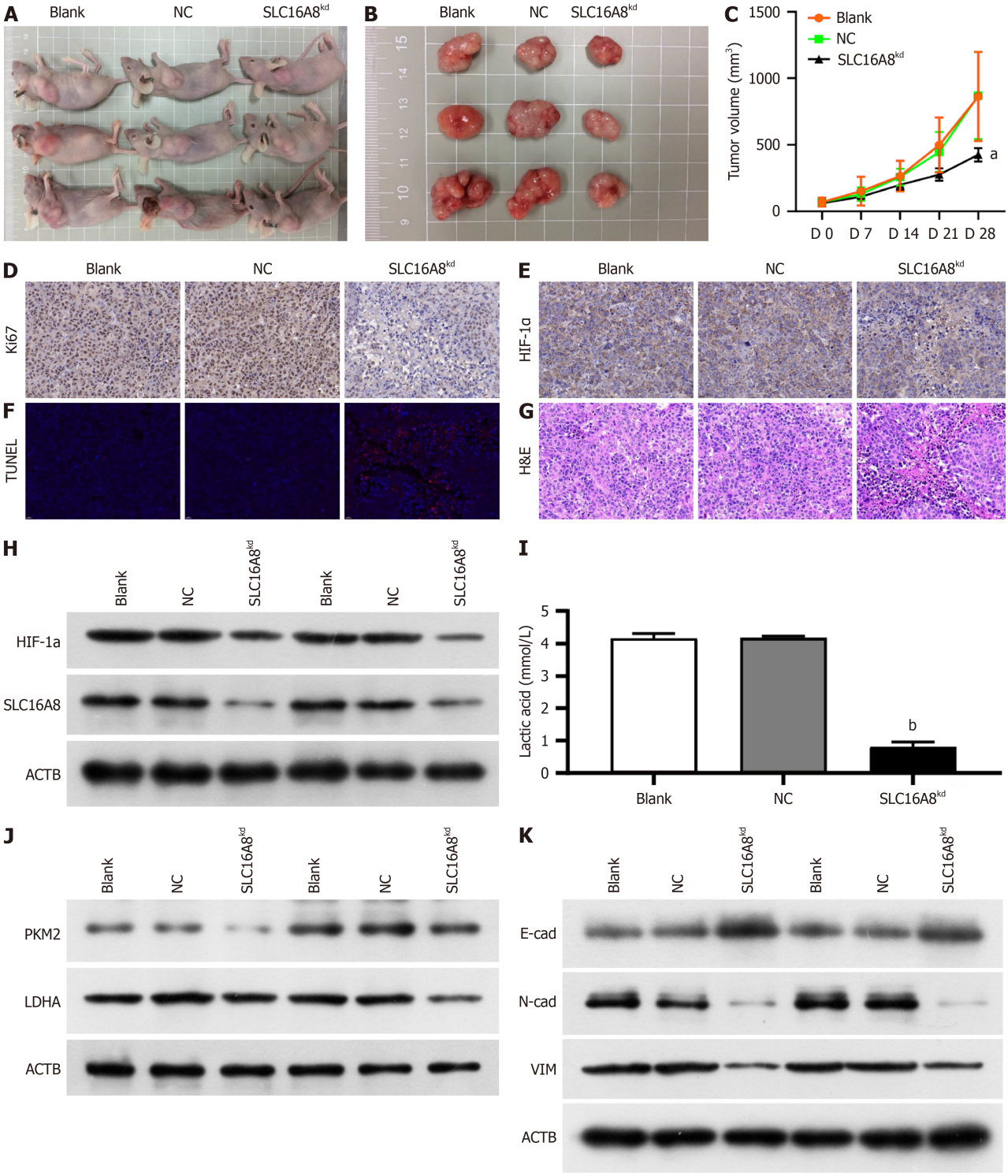

Figure 7 Effect of SLC16A8 on tumor growth. A-C: The impact of SLC16A8 knockdown on tumor growth; D: Effect of SLC16A8 knockdown on Ki67 expression in tumor; E: The effect of SLC16A8 knockdown on expression of HIF-1α and SLC16A8; F: Effect of SLC16A8 knockdown on HIF-1α expression; G: SLC16A8 knockdown promoted apoptosis in tumor; H: H&E staining was used to have a histopathological examination of tumors; I: SLC16A8 knockdown suppressed lactic acid in serum; J and K: SLC16A8 knockdown altered expression of Warburg effect- and endothelial-mesenchymal transition-related proteins' expression. $^{a}P < 0.05$, $^{b}P < 0.01$, *vs* NC.

enhances glycolysis in CRC cells.

The unique energy metabolism of malignant tumors is a vital aspect in exploring the mechanisms of tumor carcinogenesis[28]. The aberrant energy metabolism of tumors not only provides sufficient material and energy for the malignant expansion of tumors, but also plays a key role in maintaining tumor cell survival, resisting stressful stressful environments, and escaping immune suppression and metastasis[15]. Moreover, important proteins in metabolic pathways are key to control tumor metabolic activities. It has been shown that SLC16A mainly mediates the transmembrane transport of monocarboxylic acids such as lactic acid and short-chain fatty acids, and its abnormal alterations are associated with the malignant progression of various tumors[15,29]. Studies also confirmed that SLC16A8 is associated

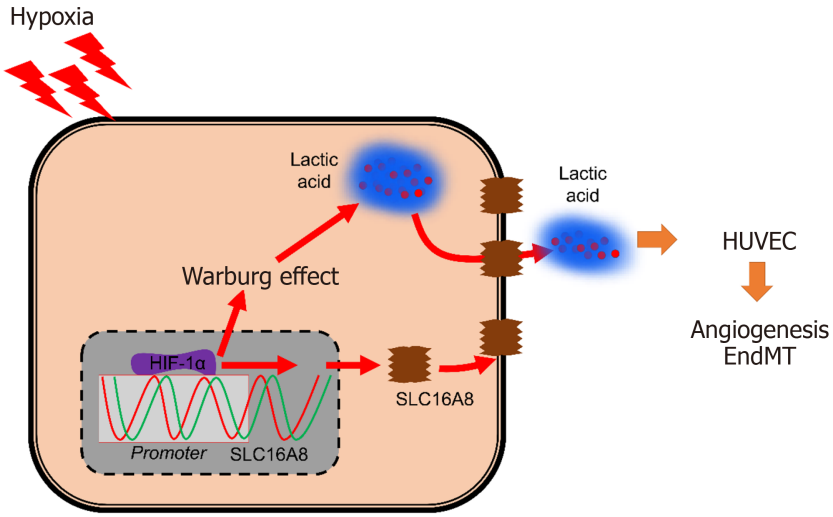

Figure 8 Graphical abstract. Under hypoxic conditions, the metabolic pathways in tumor tissues change, and lactate production increases. The expression of SLC16A8 is upregulated, causing the extrusion of lactate from cells. This leads to an increase in the distribution of tumor microvessels, providing conditions for tumor metastasis. EndMT: Endothelial-mesenchymal transition.

with impaired lactate transport in retinal pigment epithelial cells[16,30] and age-related macular degeneration[31]. In our study, we proved that SLC16A8 silencing could attenuate the proliferation, migration, invasion, angiogenesis, EMT, and glycolysis in hypoxia-induced CRC cells. And we also uncovered that SLC16A8 silencing could reduce growth, change the pathological structure, and prevent EMT and glycolysis process in CRC tumor tissues.

CONCLUSION

This study demonstrated that SLC16A8, as an oncogene, could accelerate proliferation, EMT, metastasis, angiogenesis, and glycolysis of CRC cells in the absence of oxygen. Therefore, we suggested that inhibition of SLC16A8 might weaken the Warburg effect to achieve the therapeutic effect of CRC (Figure 8).

FOOTNOTES

Author contributions: Tian HP, Peng H and Meng CY designed the experiments; Tian HP and Xiao ZX performed the experiments; Tian HP, Xiao ZX and Su BW collected the data and analyzed the data; Li YX validated the data analysis; Peng H and Meng CY provided funding support; Tian HP and Xiao ZX made equal contributions in experimental design, implementation, and data collection, and therefore are listed as co-first authors; Meng CY and Peng H are designated as co-corresponding authors due to their equal contributions in securing funding for the research project.

Supported by Nanchong Science and Technology Plan Project, No. 23JCYJPT0064; and Project of Sichuan Provincial Administration of Traditional Chinese Medicine, No. 2024MS590.

Institutional review board statement: All procedures involving clinical experiments were reviewed and approved by the Institutional Animal Care and Use Committee of the North Sichuan Medical Collage Institutional (Approval No. 2023-055).

Institutional animal care and use committee statement: The animal experiments were reviewed and approved by the North Sichuan Medical Collage Institutional Review Board (Approval No. 2021-44).

Conflict-of-interest statement: The authors declared that they had no conflicts of interest.

Data sharing statement: Dataset available from the corresponding author at p1041910523@126.com.

ARRIVE guidelines statement: The authors have read the ARRIVE guidelines, and the manuscript was prepared and revised according to the ARRIVE guidelines.

Country of origin: China

ORCID number: Hong Peng 0009-0007-2995-6881.

S-Editor: Lin C
L-Editor: A
P-Editor: Xu ZH

REFERENCES

1 **Sung H**, Ferlay J, Siegel RL, Laversanne M, Soerjomataram I, Jemal A, Bray F. Global Cancer Statistics 2020: GLOBOCAN Estimates of Incidence and Mortality Worldwide for 36 Cancers in 185 Countries. *CA Cancer J Clin* 2021; **71**: 209-249 [PMID: 33538338 DOI: 10.3322/caac.21660]
2 **Nanda N**, Dhawan DK. Role of Cyclooxygenase-2 in colorectal cancer patients. *Front Biosci (Landmark Ed)* 2021; **26**: 706-716 [PMID: 33049690 DOI: 10.2741/4914]
3 **Li J**, Ma X, Chakravarti D, Shalapour S, DePinho RA. Genetic and biological hallmarks of colorectal cancer. *Genes Dev* 2021; **35**: 787-820 [PMID: 34074695 DOI: 10.1101/gad.348226.120]
4 **Engstrand J**, Nilsson H, Strömberg C, Jonas E, Freedman J. Colorectal cancer liver metastases - a population-based study on incidence, management and survival. *BMC Cancer* 2018; **18**: 78 [PMID: 29334918 DOI: 10.1186/s12885-017-3925-x]
5 **Stewart CL**, Warner S, Ito K, Raoof M, Wu GX, Kessler J, Kim JY, Fong Y. Cytoreduction for colorectal metastases: liver, lung, peritoneum, lymph nodes, bone, brain. When does it palliate, prolong survival, and potentially cure? *Curr Probl Surg* 2018; **55**: 330-379 [PMID: 30526930 DOI: 10.1067/j.cpsurg.2018.08.004]
6 **Johdi NA**, Sukor NF. Colorectal Cancer Immunotherapy: Options and Strategies. *Front Immunol* 2020; **11**: 1624 [PMID: 33042104 DOI: 10.3389/fimmu.2020.01624]
7 **Xu J**, Meng Q, Sun H, Zhang X, Yun J, Li B, Wu S, Li X, Yang H, Zhu H, Aschner M, Relucenti M, Familiari G, Chen R. HER2-specific chimeric antigen receptor-T cells for targeted therapy of metastatic colorectal cancer. *Cell Death Dis* 2021; **12**: 1109 [PMID: 34839348 DOI: 10.1038/s41419-021-04100-0]
8 **Pavlides S**, Whitaker-Menezes D, Castello-Cros R, Flomenberg N, Witkiewicz AK, Frank PG, Casimiro MC, Wang C, Fortina P, Addya S, Pestell RG, Martinez-Outschoorn UE, Sotgia F, Lisanti MP. The reverse Warburg effect: aerobic glycolysis in cancer associated fibroblasts and the tumor stroma. *Cell Cycle* 2009; **8**: 3984-4001 [PMID: 19923890 DOI: 10.4161/cc.8.23.10238]
9 **Poff A**, Koutnik AP, Egan KM, Sahebjam S, D'Agostino D, Kumar NB. Targeting the Warburg effect for cancer treatment: Ketogenic diets for management of glioma. *Semin Cancer Biol* 2019; **56**: 135-148 [PMID: 29294371 DOI: 10.1016/j.semcancer.2017.12.011]
10 **Zanotelli MR**, Zhang J, Reinhart-King CA. Mechanoresponsive metabolism in cancer cell migration and metastasis. *Cell Metab* 2021; **33**: 1307-1321 [PMID: 33915111 DOI: 10.1016/j.cmet.2021.04.002]
11 **Boroughs LK**, DeBerardinis RJ. Metabolic pathways promoting cancer cell survival and growth. *Nat Cell Biol* 2015; **17**: 351-359 [PMID: 25774832 DOI: 10.1038/ncb3124]
12 **Zhao H**, Yang L, Baddour J, Achreja A, Bernard V, Moss T, Marini JC, Tudawe T, Seviour EG, San Lucas FA, Alvarez H, Gupta S, Maiti SN, Cooper L, Peehl D, Ram PT, Maitra A, Nagrath D. Tumor microenvironment derived exosomes pleiotropically modulate cancer cell metabolism. *Elife* 2016; **5**: e10250 [PMID: 26920219 DOI: 10.7554/eLife.10250]
13 **Halestrap AP**. The SLC16 gene family - structure, role and regulation in health and disease. *Mol Aspects Med* 2013; **34**: 337-349 [PMID: 23506875 DOI: 10.1016/j.mam.2012.05.003]
14 **Felmlee MA**, Jones RS, Rodriguez-Cruz V, Follman KE, Morris ME. Monocarboxylate Transporters (SLC16): Function, Regulation, and Role in Health and Disease. *Pharmacol Rev* 2020; **72**: 466-485 [PMID: 32144120 DOI: 10.1124/pr.119.018762]
15 **Bosshart PD**, Charles RP, Garibsingh RA, Schlessinger A, Fotiadis D. SLC16 Family: From Atomic Structure to Human Disease. *Trends Biochem Sci* 2021; **46**: 28-40 [PMID: 32828650 DOI: 10.1016/j.tibs.2020.07.005]
16 **Klipfel L**, Cordonnier M, Thiébault L, Clérin E, Blond F, Millet-Puel G, Mohand-Saïd S, Goureau O, Sahel JA, Nandrot EF, Léveillard T. A Splice Variant in SLC16A8 Gene Leads to Lactate Transport Deficit in Human iPS Cell-Derived Retinal Pigment Epithelial Cells. *Cells* 2021; **10** [PMID: 33477551 DOI: 10.3390/cells10010179]
17 **Dekker E**, Tanis PJ, Vleugels JLA, Kasi PM, Wallace MB. Colorectal cancer. *Lancet* 2019; **394**: 1467-1480 [PMID: 31631858 DOI: 10.1016/S0140-6736(19)32319-0]
18 **Biller LH**, Schrag D. Diagnosis and Treatment of Metastatic Colorectal Cancer: A Review. *JAMA* 2021; **325**: 669-685 [PMID: 33591350 DOI: 10.1001/jama.2021.0106]
19 **Multhoff G**, Vaupel P. Hypoxia Compromises Anti-Cancer Immune Responses. *Adv Exp Med Biol* 2020; **1232**: 131-143 [PMID: 31893404 DOI: 10.1007/978-3-030-34461-0_18]
20 **Yuen VW**, Wong CC. Hypoxia-inducible factors and innate immunity in liver cancer. *J Clin Invest* 2020; **130**: 5052-5062 [PMID: 32750043 DOI: 10.1172/JCI137553]
21 **Infantino V**, Santarsiero A, Convertini P, Todisco S, Iacobazzi V. Cancer Cell Metabolism in Hypoxia: Role of HIF-1 as Key Regulator and Therapeutic Target. *Int J Mol Sci* 2021; **22** [PMID: 34071836 DOI: 10.3390/ijms22115703]
22 **Sebestyén A**, Kopper L, Dankó T, Tímár J. Hypoxia Signaling in Cancer: From Basics to Clinical Practice. *Pathol Oncol Res* 2021; **27**: 1609802 [PMID: 34257622 DOI: 10.3389/pore.2021.1609802]
23 **Mulukutla BC**, Yongky A, Le T, Mashek DG, Hu WS. Regulation of Glucose Metabolism - A Perspective From Cell Bioprocessing. *Trends Biotechnol* 2016; **34**: 638-651 [PMID: 27265890 DOI: 10.1016/j.tibtech.2016.04.012]
24 **Bose S**, Le A. Glucose Metabolism in Cancer. *Adv Exp Med Biol* 2018; **1063**: 3-12 [PMID: 29946772 DOI: 10.1007/978-3-319-77736-8_1]
25 **Lu YY**, Wu CH, Hong CH, Chang KL, Lee CH. GLUT-1 Enhances Glycolysis, Oxidative Stress, and Fibroblast Proliferation in Keloid. *Life (Basel)* 2021; **11** [PMID: 34070830 DOI: 10.3390/life11060505]
26 **Bergers G**, Fendt SM. The metabolism of cancer cells during metastasis. *Nat Rev Cancer* 2021; **21**: 162-180 [PMID: 33462499 DOI:

10.1038/s41568-020-00320-2]

27 **Schwartz L**, Supuran CT, Alfarouk KO. The Warburg Effect and the Hallmarks of Cancer. *Anticancer Agents Med Chem* 2017; **17**: 164-170 [PMID: 27804847 DOI: 10.2174/1871520616666161031143301]

28 **Zhang Y**, Yang JM. Altered energy metabolism in cancer: a unique opportunity for therapeutic intervention. *Cancer Biol Ther* 2013; **14**: 81-89 [PMID: 23192270 DOI: 10.4161/cbt.22958]

29 **Yu S**, Wu Y, Li C, Qu Z, Lou G, Guo X, Ji J, Li N, Guo M, Zhang M, Lei L, Tai S. Comprehensive analysis of the SLC16A gene family in pancreatic cancer *via* integrated bioinformatics. *Sci Rep* 2020; **10**: 7315 [PMID: 32355273 DOI: 10.1038/s41598-020-64356-y]

30 **Daniele LL**, Sauer B, Gallagher SM, Pugh EN Jr, Philp NJ. Altered visual function in monocarboxylate transporter 3 (Slc16a8) knockout mice. *Am J Physiol Cell Physiol* 2008; **295**: C451-C457 [PMID: 18524945 DOI: 10.1152/ajpcell.00124.2008]

31 **Cascella R**, Strafella C, Longo G, Ragazzo M, Manzo L, De Felici C, Errichiello V, Caputo V, Viola F, Eandi CM, Staurenghi G, Cusumano A, Mauriello S, Marsella LT, Ciccacci C, Borgiani P, Sangiuolo F, Novelli G, Ricci F, Giardina E. Uncovering genetic and non-genetic biomarkers specific for exudative age-related macular degeneration: significant association of twelve variants. *Oncotarget* 2018; **9**: 7812-7821 [PMID: 29487693 DOI: 10.18632/oncotarget.23241]

Published by **Baishideng Publishing Group Inc**
7041 Koll Center Parkway, Suite 160, Pleasanton, CA 94566, USA
Telephone: +1-925-3991568
E-mail: office@baishideng.com
Help Desk: https://www.f6publishing.com/helpdesk
https://www.wjgnet.com